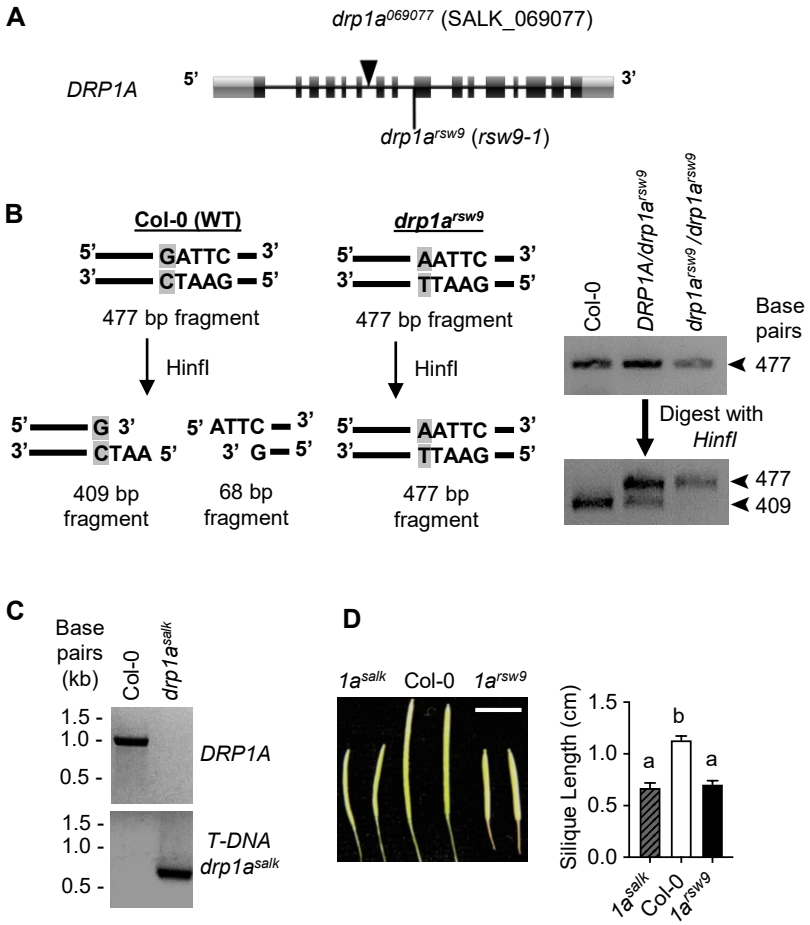

Supplemental Figure S1. Isolation and confirmation of *drp1a* mutant alleles.

A, Gene structure of *DRP1A* (*At5g42080*). Position of T-DNA insertional allele (black arrowhead) and position of point mutation (black mark) relative to coding sequence (black bars), introns (black lines), and 5' and 3' untranslated region (gray bar). B, CAPS analysis to identify *drp1a*^{rsw9} homozygous mutant plants. Due to the presence of a *HinfI* restriction site (▼) in Col-0 (at2314 bp) but not *drp1a*^{rsw9}, digesting PCR products with *HinfI* restriction enzyme resulted in a smaller size fragments for wild-type *DRP1A* (409 bp) and a larger size fragment for *drp1a*^{rsw9} (477 bp). C, PCR genotyping using gene specific primers for *DRP1* confirmed the isolation of homozygous *drp1a*^{069077} line (SALK_069077). D, Representative images of matured siliques of *drp1a*^{salk} (*1a*^{salk}), Col-0 and *drp1a*^{rsw9} (*1a*^{rsw9}); Scale bar = 5mm. E, Quantification of matured silique length measured using Fiji open source software (n = 10). Values are means ± SE; and different letters denote statistically significant difference and same letter indicate no significant difference based on Ordinary one-way ANOVA ($p < 0.05$). Experiments were repeated at least 3 times with similar results using biologically distinct samples for each biological replicate. kb, kilobase; bp, base pair; Col-0, wild-type; *1a*^{salk}, *drp1a*^{069077}; *1a*^{rsw9}, *drp1a*^{rsw9}.

Supplemental Figure S2. Loss of *DRP1A* results in reduced rosette leaf size compared to *drp2b* and Col-0 plants.

Rosette leaves of both independent *drp1a*^{salk} and *drp1a*^{rsw9} mutant alleles were smaller than Col-0 and *drp2b-2* in 5- to 6-week-old plants grown for pathogen and flg22-assays. Scale bar = 2 cm. Rosettes of different genotypes were digitally extracted from the same image and aligned for comparison. Experiment was repeated at least 3 times with similar results using biologically distinct samples for each biological replicate. Col-0, wild-type*;* *drp1a*^{salk}, *drp1a*^{069077}.

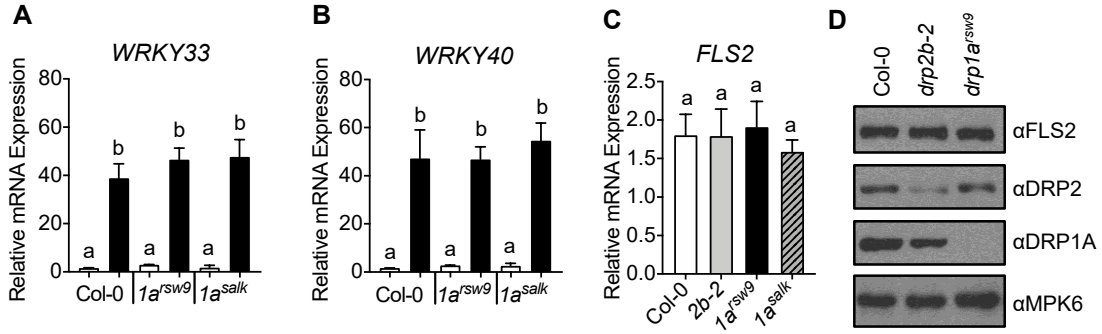

Supplemental Figure S3. *drp1a* mutant plants show similar accumulation of *WRKY33* mRNA, *WRKY40* mRNA, *FLS2* mRNA and FLS2 protein to Col-0.

A and B, For *WRKY33* mRNA and *WRKY40* mRNA, 0.1 µM flg22 was infiltrated for 0 min (□) or 30 min (■) into leaves of 5-to 6-week-old Col-0 or *drp1* mutant plants. n = 3 biological samples/genotype/treatment as described in Fig. 3. C, Steady-state accumulation of *FLS2* mRNA. n = 6 biological samples/genotype. For A-C, each n consisted of 3 leaf punches collected from 1 to 2 plants. Relative mRNA levels for each gene were measured using RT-qPCR and normalized to the reference *SAND* gene *At2g28390*. Values are means ± SE with different letters indicating statistically significant differences, and the same letter indicating no statistically significant difference based on one-way ANOVA ($p < 0.05$). D, Immunoblot analysis of steady-state FLS2 protein levels. Total protein extracts from leaves of 5-6 weeks old Col-0, *drp2b* and *drp1a* mutants were probed by immunoblot analysis with antibodies against FLS2. αDRP2 antibody confirmed reduced DRP2 protein accumulation in *drp2b-2* with the residual DRP2 protein detected by the αDRP2 antibody corresponding to the close paralog DRP2A. αDRP1A antibody confirmed no detectable DRP1A protein accumulation in *drp1a*^{rsw9} mutant. MPK6 antibody served as loading control. Each experiment was performed at least three times with similar results using biologically distinct samples for each biological replicate. Col-0, wild-type (white bar); *1a*^{rsw9}, *drp1a*^{rsw9} (black bar); *1a*^{salk}, *drp1a*^{069077} (gray bar with black stripes) and *2b-2*, *drp2b-2* (gray bar).

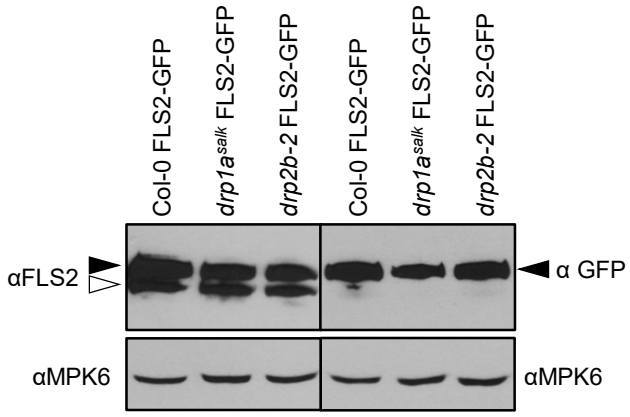

Supplemental Figure S4. FLS2-GFP and endogenous FLS2 protein accumulation is similar in *drp1a* and Col-0 seedlings.

Using immunoblot analysis, total protein extracts from 7-day-oldseedlings of *drp1a*^{salk} FLS2-GFP, *drp2b-2* FLS2-GFP and Col-0 FLS2-GFP were probed with αFLS2 and αGFP antibodies. αFLS2 antibody detected both endogenous FLS2 (white arrowhead) and FLS2-GFP (black arrowhead). αGFP antibody detects FLS2-GFP (black arrowhead). αMPK6 served as a loading control. The experiment was repeated three times with similar results using biologically distinct samples for each biological replicate. Col-0, wild-type.

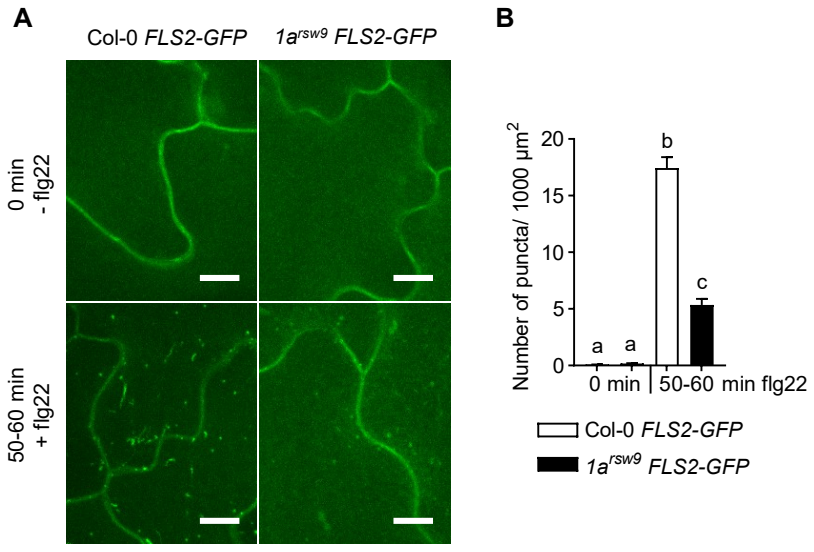

Supplemental Figure S5. Similar to *drp1a*^{salk}, cotyledons of *drp1a*^{rsw9} mutant seedlings show impaired flg22-induced endocytosis of FLS2-GFP.

For A and B, Col-0 *FLS2-GFP* (WT) and *drp1a*^{rsw9} *FLS2-GFP* (*1a*^{rsw9} *FLS2-GFP*) seedlings were treated with 1 µM flg22 for 0 and 50-60 min to examine for ligand-induced endocytosis in adaxial surface of cotyledon epidermis using SDCM. A, Representative maximum-intensity projection images of FLS2-GFP fluorescence. Scale bars = 10 µm. B, Quantification of FLS2-GFP puncta at indicated times post-elicitation with n ≥ 18 images/genotype/treatment with at least 6 images each taken from 3 different seedling per genotype and treatment. Values are means ± SE. different letters denote statistically significant difference and with same letter indicating no statistically significant difference based on Ordinary one-way ANOVA ($p < 0.05$). Experiment was repeated five times with similar results using biologically distinct samples for each biological replicate. Min; minutes.

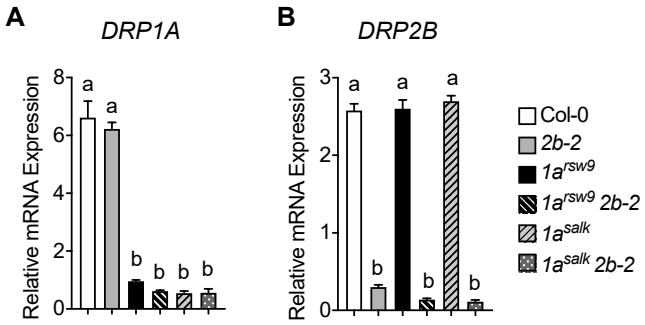

Supplemental Figure S6. Steady-state accumulation of *DRP1A* and *DRP2B* mRNA in *drp* single and double mutant seedlings.

A and B, Using RT-qPCR, steady-state *DRP1A* mRNA (A) and *DRP2B* mRNA (B) was measured in 7-day-old seedlings and normalized to the reference *SAND* gene *At2g28390*. n = 3-4 samples/genotype, with each biological sample (n) containing 4 seedlings for Col-0 and single *drp* mutants and 15 seedlings for double mutants. Values are means ± SE with different letters indicating statistically significant differences and with same letter indicating no statistically significant difference based on one-way ANOVA ($P < 0.05$). Each experiment was repeated at least 5 times with similar results using biologically distinct samples for each biological replicate. Col-0, wild-type (white bar); *1a*^{rsw9}, *drp1a*^{rsw9} (black bar); *1a*^{salk}, *drp1a*^{069077} (gray bar with black stripes), *2b-2*, *drp2b-2* (gray bar), *1a*^{rsw9} *2b-2*, *drp1a*^{rsw9} *drp2b-2* (black bar with white stripes); and *1a*^{salk} *2b-2*, *drp1a*^{069077} *drp2b-2* (gray bar with white dots).

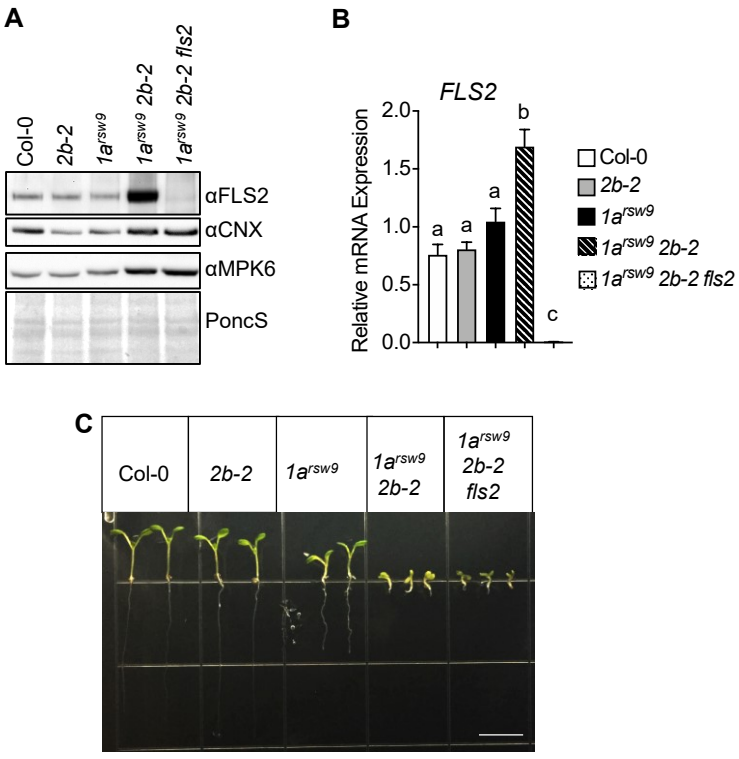

Supplemental Figure S7. *drp1a drp2b* double mutants hyperaccumulate FLS2 protein and *FLS2* mRNA

A, Using immunoblot analysis, total protein extracts from 7-day-old seedlings were probed with αFLS2 antibodies. αMPK6, αCNX and PonceauS served as loading controls. B, Using RT-qPCR, steady-state *FLS2* mRNA was measured in 7-day-old seedlings and normalized to the reference *SAND* gene *At2g28390*. n = 3-4 samples/genotype, with each biological sample (n) containing 4 seedlings for Col-0 and single *drp* mutants and 15 seedlings for *drp* double and triple mutants. C, representative image of 7-day-old seedlings showing that additional loss of *FLS2* did not suppress the stunted seedling growth of the *drp1a drp2b* double mutant. Scale bar = 5 mm. Values are means ± SE with different letters indicating statistically significant differences and with same letter indicating no statistically significant difference based on one-way ANOVA ($P < 0.05$). Each experiment was repeated at least 3 times with similar results using biologically distinct samples for each biological replicate. CNX, CALNEXIN1/2; PoncS, PonceauS; Col-0, wild-type (white bar); *1a*^{rsw9}, *drp1a*^{rsw9} (black bar); *2b-2*, *drp2b-2* (gray bar), *1a*^{rsw9} *2b-2*, *drp1a*^{rsw9} *drp2b-2* (black bar with white stripes); and *1a*^{rsw9} *2b-2 fls2*, *drp1a*^{rsw9} *drp2b-2 fls2⊿* (white bar with black dots).

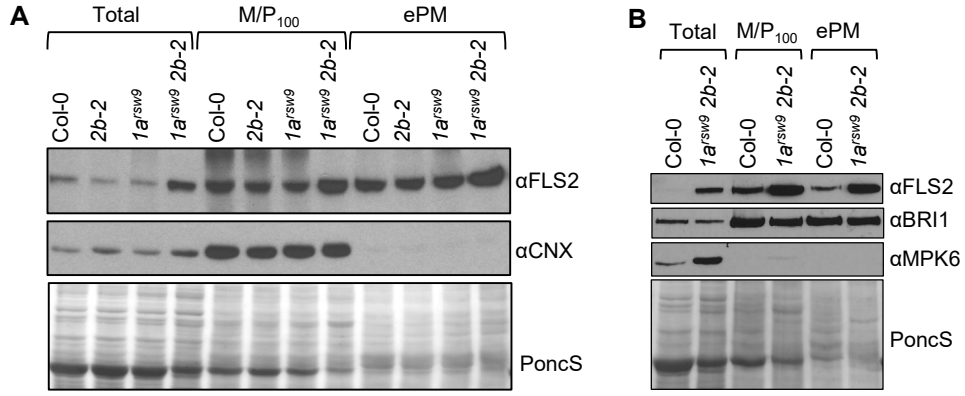

Supplemental Figure S8. Combinatorial loss of *DRP1A* and *DRP2B* results in hyperaccumulation of FLS2 but not BRI1.

A, Immunoblot analysis of Total, M/P100, and ePM protein fractions from in 7-to-8-day-old *drp1a*^{rsw9}, *drp2b-2*, *drp1a*^{rsw9} *drp2b-2* and Col-0 seedlings were probed with FLS2 antibodies. CALNEXIN1/2 (CNX) served as ER membrane marker protein. B, Immunoblot analysis of Total, M/P_{100}, and ePM protein fractions from *drp1a*^{rsw9} *drp2b-2* and Col-0 were probed with FLS2 and BRI1 antibodies. MPK6 served as soluble marker protein. PoncS served as loading control. Each experiment was repeated at least three times with similar results using biologically distinct samples for each biological replicate. Col-0, wild-type; *1a*^{rsw9}, *drp1a*^{rsw9}; *2b-2*, *drp2b-2; 1a*^{rsw9} *2b-2*, *drp1a*^{rsw9} *drp2b-2;* M/P_{100}, Microsomes/Pellet100; ePM, enriched plasma membrane, PoncS, Ponceau S.

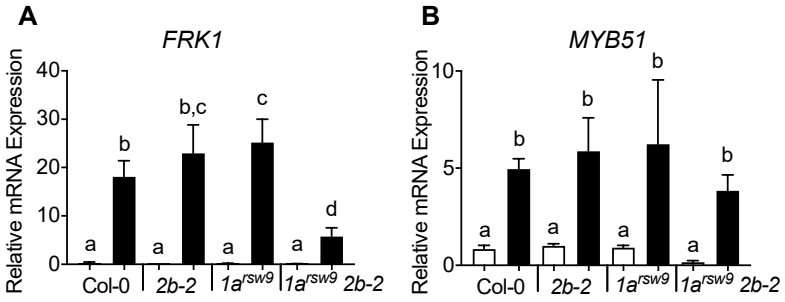

Supplemental Figure S9. Combinatorial loss of *DRP1A* and *DRP2B* results in reduced *FRK1* but not *MYB51* mRNA accumulation in response to flg22.

A and B, 7-day-old seedlings of Col-0, *drp2b-2*, *drp1a*^{rsw9}, *drp1a*^{rsw9} *drp2b-2* were treated with 1 µM flg22 for 0 h (□) or 2 h (■). Using RT-qPCR was measured for *FRK1* (A) and *MYB51* (B) mRNA and normalized to the reference *SAND* gene *At2g28390.* n = 4 samples/genotype for +flg22 and n = 3 samples/genotype for –flg22. Each sample (n) consisted of 4 seedlings/sample for Col-0, *drp2b* and *drp1a* single mutants and 15 seedlings/sample for *drp1a drp2b* double mutants. Values are means ± SE with different letters indicating statistically significant differences and with same letter indicating no statistically significant difference based on one-way ANOVA. All experiments were performed at least 3 times with similar results using biologically distinct samples for each biological replicate. Col-0, wild-type; *1a*^{rsw9}, *drp1a*^{rsw9}; *2b-2*, *drp2b-2; 1a*^{rsw9} *2b-2*, *drp1a*^{rsw9} *drp2b-2.*

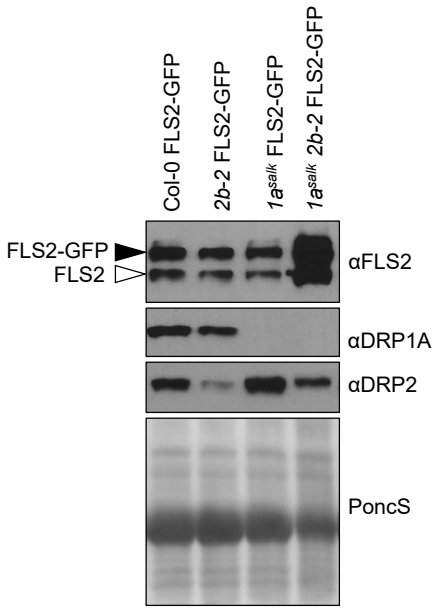

Supplemental Figure S10. FLS2-GFP and endogenous FLS2 proteins hyperaccumulate in *drp1a^{salk} drp2b-2* FLS2-GFP mutant lines.

For *drp1a^{salk} drp2b-2* FLS2-GFP*, drp1a^{salk}* FLS2-GFP, *drp2b-2* FLS2-GFP and Col-0 FLS2-GFP*,* total protein extracts from 7-day-old seedlings were probed with αDRP1A, αDRP2 and αFLS2 antibodies. PoncS serve as a loading control. αFLS2 antibody detects both endogenous FLS2 (white arrowhead) and FLS2-GFP (black arrowhead). All experiments were performed 3 times with similar results using biologically distinct samples for each biological replicate. Col-0 FLS2-GFP, Col-0; *1a^{salk} 2b-2* FLS2-GFP*, drp1a^{069077} drp2b-2* FLS2-GFP*; 1a^{salk}* FLS2-GFP, *drp1a^{069077}* FLS2-GFP; *2b-2* FLS2-GFP, *drp2b-2* FLS2-GFP; PoncS, Ponceau S.

Supplemental Table S1. Primer list. List of oligonucleotide sequences used as primers.

Purpose	Primer Name	Sequence (5'-3')	Cycle	References
CAPS	DRP1A^{rsw9} Short F	ATCTTGCTACCTCAGATGCA	30	Collings *et al*., 2008
CAPS	DRP1A^{rsw9} Short R	ATCTGCTTGGGAACGGTTGA	30	Collings *et al*., 2008
genotyping	drp1a^{salk} F	CTTACTTCCACTGCATCCGTC	30	This study
genotyping	drp1a^{salk} R	AGAGTTTCTTCACCTCCCGAG	30	This study
genotyping	drp2b-2-LP	ATAGCCTAATTGGGCATCCAG	30	Backues *et al*., 2010
genotyping	drp2b-2-RP	TATAGCATCGTTGTGCTGTGC	30	Backues *et al*., 2010
genotyping	FLS2-3xMyc-EGFP F	AAACTTGGAGGACACCATTCAC	30	Smith *et al*., 2014a
genotyping	FLS2-3xMyc-EGFP R	TGTTCACCGTTCAAGTCTTCCTC	30	Smith *et al*., 2014a
genotyping	LBb1	GCGTGGACCGCTTGCTGCAACT	30	Smith *et al*., 2014a
RT-qPCR	At2g28390 F	AACTCTATGCAGCATTTGATCCACT	40	Korasick *et al*., 2010
RT-qPCR	At2g28390 R	TGATTGCATATCTTTATCGCCATC	40	Korasick *et al*., 2010
RT-qPCR	DRP1A F	AGCAAGGTTACCGTCGTCTC	40	This study
RT-qPCR	DRP1A R	AGATAGCATGAACGGTGTCAAC	40	This study
RT-qPCR	DRP2B F	GTGAACATGCACAGCACAAC	40	This study
RT-qPCR	DRP2B R	GCTGCCTGATCAATTTTGCTG	40	This study
RT-qPCR	FLS2 F	TCTGATGAAACTTAGAGGCAAAGCG	40	Smith *et al*., 2014b
RT-qPCR	FLS2 R	CGTAACAGAGTTTGGCAAAGTCG	40	Smith *et al*., 2014b
RT-qPCR	MYB51 F	ACGTGTTCTTCGTCCACG	40	Orosa *et al*., 2018
RT-qPCR	MYB51 R	TAGACCGGCGTCACATC	40	Orosa *et al*., 2018
RT-qPCR	PHI1 F	TTGGTTTAGACGGGATGGTG	40	Smith *et al*., 2014a
RT-qPCR	PHI1 R	ACTCCAGTACAAGCCGATCC	40	Smith *et al*., 2014a
RT-qPCR	PR1 F	GCAATGGAGTTTGTGGTCAC	40	Korasick *et al*., 2010
RT-qPCR	PR1 R	GTTCACATAATTCCCACGAGG	40	Korasick *et al*., 2010
RT-qPCR	WRKY33 F	AGCAAAGAGATGGAAAGGGGACAA	40	Smith *et al*., 2014a
RT-qPCR	WRKY33 R	GCACTACGATTCTCGGCTCTCTCA	40	Smith *et al*., 2014a
RT-qPCR	WRKY40 F	TGCGAGTTGAAGAAGATCCACCGA	40	Smith *et al*., 2014a
RT-qPCR	WRKY40 R	TCCGAGAGCTTCTTGTTCTCAGCA	40	Smith *et al*., 2014a